

# Miscibility and phase behavior in blends of phenolphthalein poly(ether sulfone) and poly(hydroxyether of bisphenol A)

Sixun Zheng<sup>a,b</sup>, Qipeng Guo<sup>c</sup>, Yongli Mi<sup>a,\*</sup>

<sup>a</sup>*Department of Chemical Engineering, The Hong Kong University of Science and Technology, Clear Water Bay, Kowloon, Hong Kong, People's Republic of China*

<sup>b</sup>*Department of Polymer Science and Engineering, Shanghai Jiao Tong University, Shanghai 200240, People's Republic of China*

<sup>c</sup>*Department of Polymer Science and Engineering, University of Science and Technology of China, Hefei 230026, People's Republic of China*

Received 22 April 2002; received in revised form 24 September 2002; accepted 10 October 2002

## Abstract

Miscibility and phase behavior in the blends of phenolphthalein poly(ether sulfone) (PES-C) with poly(hydroxyether of bisphenol A) (PH) were investigated by means of differential scanning calorimetry (DSC), high resolution solid state nuclear magnetic resonance spectroscopy (NMR) and Fourier transform infrared spectroscopy (FTIR). It was found that the homogeneity of the as-prepared blends depended on the solvents used; *N,N*-dimethylformamide (DMF) provided the segmental mixing for PH and PES-C, which is confirmed by the behavior of single, composition-dependent glass transition temperatures ( $T_g$ 's). To examine the homogeneity of the blends at the molecular level, the proton spin–lattice relaxation times in the rotating frame  $T_{1\rho}(H)$  were measured via  $^{13}\text{C}$  CP/MAS NMR spectroscopy as a function of blend composition. In view of the  $T_{1\rho}(H)$  values, it is concluded that the PH and PES-C chains are intimately mixed on the scale of 20–30 Å. FTIR studies indicate that there were the intermolecular specific interactions in this blends, involved with the hydrogen-bonding between the hydroxyls of PH and the carbonyls of PES-C, and the strength of the intermolecular hydrogen bonding is weaker than that of PH self-association. At higher temperature, the PH/PES-C blends underwent phase separation. By means of thermal analysis, the phase boundaries of the blends were determined, and the system displayed the lower critical solution temperature behavior. Thermogravimetry analysis (TGA) showed that the blends exhibited the improved thermal stability, which increases with increasing PES-C content.

© 2002 Elsevier Science Ltd. All rights reserved.

**Keywords:** Poly(hydroxyether of bisphenol A); Phenolphthalein poly(ether sulfone); Miscibility

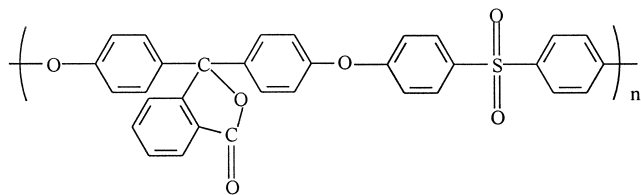
## 1. Introduction

Polymer blends have played the important roles in the development of new materials with designed properties during the past decades [1,2]. Recently, much importance was attached to the studies of polymer blends comprising high-performance thermoplastics due to the potential application of these engineering materials. An important objective of these studies is to improve mechanical properties and processability and to establish the balance between the properties and economic advantage through the synergistic contribution of blend component [2]. The properties of polymer blends depend on the mixing degree of constituent polymers, and thus it is essential to investigate the

miscibility and phase behavior of blend systems [1–4]. A variety of techniques have been employed to investigate miscibility and phase behavior of polymer blends, including thermal, mechanical and electric analysis, light scattering, microscopy and spectroscopy [1–4]. Solid state NMR spectroscopy was proved to be powerful to characterize phase structure of polymer blends at the molecular level by providing information on microstructure of blends and dynamics of macromolecular chain relaxation. In terms of spin diffusion mechanism, dynamic relaxation parameters of protons in the rotating frame ( $T_{1\rho}(H)$ ) of a multi-component system are strongly dependent of the short range spatial proximity (1 nm) since the effect of spin diffusion on  $T_{1\rho}(H)$  relaxation can reveal the way in which an efficiently relaxing entity can further relax other entities in the polymer blend systems. This approach is considered to be the NMR criterion for miscibility in polymer blend systems [5–15].

\* Corresponding author. Tel.: +852-2358-7127; fax: +852-2358-0054.  
E-mail address: keymix@ust.hk (Y. Mi).

Phenolphthalein poly(ether sulfone) (PES-C) is a newly developed engineering thermoplastic [16] and it has been identified as a high-performance polymer. It has widely been used as the matrices of polymer composites due to its excellent mechanical and thermal properties. In the viewpoint of chemical structure, PES-C can be taken as a modified poly(ether sulfone) (PES), and its repeat unit is schemed as follows:



The introduction of the rather bulky and polarizable phenolphthalein group in place of aromatic ring results in an increased rigidity of the molecular chain, thus the higher glass transition temperature ( $\sim 255^\circ\text{C}$ ) was displayed. A few studies of PES-C blends with several other polymers were previously reported [17–22]. PES-C was found to be fully miscible with poly(ethylene oxide) (PEO) and the blends possess lower critical solution temperature (LCST) behavior [21]. PES-C was also exploited to modify epoxy resins [22]. In this contribution, we present a study of amorphous engineering polymer blends composed of PES-C and poly(hydroxyether of bisphenol A) (PH). The miscibility, specific intermolecular interaction, phase behavior and thermal properties of the blends were addressed on the basis of differential scanning calorimetry (DSC), solid state  $^{13}\text{C}$  nuclear magnetic resonance spectroscopy (NMR), Fourier transform infrared spectroscopy (FTIR), and thermogravimetric analysis (TGA).

## 2. Experimental

### 2.1. Materials and preparation of samples

Phenolphthalein poly(ether sulfone) (PES-C) used is supplied by Xuzhou Engineering Plastics Co, Xuzhou, China. Its glass transition temperature ( $T_g$ ) is  $255^\circ\text{C}$ . It has a reduced solution viscosity of 0.68 dl/g. GPC measurement indicates that the polymer possesses the molecular weight of  $M_n = 31\,000$  and  $M_w/M_n = 1.65$ . Poly(hydroxyether of bisphenol A) (PH) was synthesized in this laboratory, and it has the average molecular weight of  $M_n = 33\,000$  and  $M_w/M_n = 2.1$ . All these values of molecular weight were expressed as standard PS equivalent molecular weight in GPC measurement.

The PH/PES-C blends were prepared by solution casting from chloroform at room temperature and from *N,N*-dimethylformamide (DMF) at  $50^\circ\text{C}$ , respectively. The total polymer concentration was controlled within 5%

(w/v). To remove the residual solvent, all the blend films were further desiccated in vacuo at  $60^\circ\text{C}$  for 2 weeks.

### 2.2. Techniques and measurements

#### 2.2.1. Differential scanning calorimetry

The calorimetric measurements were performed on a Du Pont TA 2190 differential scanning calorimeter in a dry nitrogen atmosphere. The instrument was calibrated with standard Indium. The samples (about 5 mg in weight) were first heated up to the temperature between phase separation and glass transition and held for 5 min to remove the thermal history, followed by quenching to  $-20^\circ\text{C}$ . A heating rate of  $20^\circ\text{C}/\text{min}$  was used in all cases. Glass transition temperature ( $T_g$ ) was taken as the midpoint of the heat capacity change.

Phase separation process was investigated by means of DSC. The samples were first annealed at the selected temperature for 10 min, and then quenched to  $0^\circ\text{C}$ . The heating scans were recorded. Then the sample was annealed at the next higher temperature for 10 min, and quenched. The higher temperature was changed by  $10^\circ\text{C}$  intervals. This procedure was repeated until the occurrence of phase separation is observed. The annealing temperature corresponding to the first change of glass transition was taken as the phase separation temperature.

#### 2.2.2. $^{13}\text{C}$ cross-polarization (CP)/magic angle spinning (MAS) nuclear magnetic resonance spectroscopy

Solid state NMR experiments were carried out at ambient temperature ( $27^\circ\text{C}$ ) on a Jeol JNM-EX400 FT NMR spectrometer at the resonance frequencies of 399.65 MHz for proton. The high-resolution  $^{13}\text{C}$  NMR spectra were obtained using CP/MAS together with the high-power dipolar decoupling (DD) technique. The  $90^\circ$ -pulse width of  $5.5\ \mu\text{s}$  was employed with free induction decay signal accumulation, and the CP Hartmann–Hahn contact time was set at 1.0 ms for all experiments. The rate of MAS was 4.9–5.1 kHz for measuring  $^{13}\text{C}$  spectra and relaxation time. The Hartmann–Hahn CP matching and DD field was 40 kHz. The chemical shifts of all  $^{13}\text{C}$  spectra were determined by taking the carbon of solid adamantane (29.5 ppm relative to tetramethyl silane, TMS) as an external reference standard.

The proton spin–lattice relaxation times in the rotating frame  $T_{1\rho}(\text{H})$  were determined by observing the carbon signal intensities with a  $^1\text{H}$  matched spin-lock- $\tau$  pulse sequence prior to CP (Fig. 1(a)). For the assignment of  $^{13}\text{C}$  CP/MAS spectrum of PES-C, the dipolar dephasing experiment was carried out to eliminate CH and  $\text{CH}_2$  resonance leaving the resonance lines of quaternary and methyl carbons, and the pulse sequence is shown in Fig. 1(b).

#### 2.2.3. Fourier transform infrared spectroscopy

The thin films of PH, PES-C and their blend films were

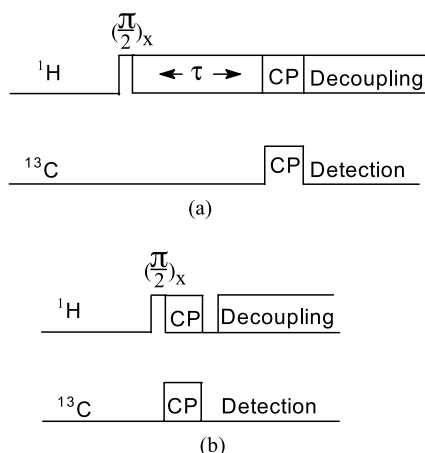


Fig. 1. The pulse sequences used in this work. (a)  $T_{1\rho}(\text{H})$  measurement, (b) dipolar dephasing experiment. The dephasing interval is 50  $\mu\text{s}$ .

cast from 2 wt% DMF at 60 °C. The films obtained were dried at 60 °C for 2 weeks to remove residual solvent. All of casting films used in the study were sufficiently thin to be within a range where the Beer–Lambert law is obeyed. All infrared measurements were performed on a Bio-FTR spectrometer at room temperature (27 °C). One-hundred and twenty eight scans at resolution of 2  $\text{cm}^{-1}$  were used to record the spectra.

#### 2.2.4. Optical microscopy

The Leica-LMP optical microscope equipped with a hot stage was used for cloud point measurement. The films with various composition of blend were heated at a rate of 5 °C/min through the cloud points, and the cloud point was defined as the onset of the turbidity. The cloud points was plotted as a function of blend composition.

#### 2.2.5. Thermogravimetry analysis

The TA 2950 thermogravimetric analyzer was used to investigate the thermal degradation of blends. The samples (about 10 mg) were heated under a nitrogen atmosphere from ambient temperature. The heating rate of 10 °C/min was used in all cases. The thermal degradation temperature was taken as the onset temperature of the thermal decomposition.

### 3. Results and discussion

#### 3.1. Miscibility of blends

##### 3.1.1. Differential scanning calorimetry

All the PH/PES-C blend films casting from chloroform were cloudy at room temperature and at elevated temperatures, suggesting the formation of phase-separated structure, which was confirmed by DSC traces, in which, all the DSC curves displayed two separate glass transition temperatures ( $T_g$ 's). However, the transparent films of the PH/PES-C

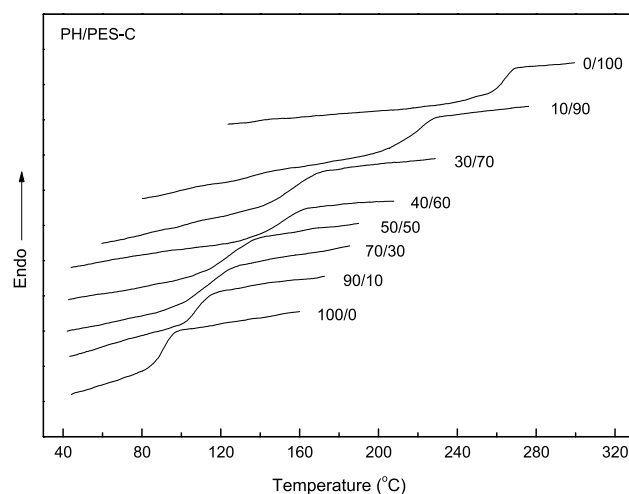


Fig. 2. DSC thermograms of PH/PES-C blends.

blends were obtained when cast from DMF. The clarity indicates that all the blends are homogeneous, i.e. phase separation did not occur at least on a scale exceeding the wavelength of visible light. Further heated up to elevated temperatures, all the clear samples became cloudy in succession. Careful microscopic observations of these cloudy films showed the obvious phase-separated structure. These phenomena suggest that the PH/PES-C blends exhibited the LCST behavior. It was noted that phase behavior of the system is quite dependent on the selection of casting solvents. The ‘solvent effect’ on the homogeneity of casting polymer blend films has previously been interpreted in terms of the difference in the two polymer–solvent interaction parameters  $|\chi_{12} - \chi_{13}|$  or  $|\Delta\chi|$  (herein subscript 1 referring to solvent whereas subscript 2 (or 3) standing for polymer). From a ternary phase diagram, a homogeneous system is attained only with a suitably small  $|\Delta\chi|$ , in addition, a small polymer–polymer interaction parameter  $\chi_{23}$  is necessary [23–28]. The transparent blend films prepared via DMF were used throughout this study.

All the blends were subjected to the thermal analysis. Shown in Fig. 2 are the DSC curves of the PH/PES-C blends. It is seen that each blend displayed a single glass transition temperature ( $T_g$ ), intermediate between those of the two pure components and changing with the blend composition. In view of the transparency and glass transition behavior, the conclusion can be reached that the PH/PES-C blends are completely miscible in the amorphous state, i.e. possess single, homogeneous phases. Fig. 3 summarises the plot of the glass transition temperatures ( $T_g$ 's) of the blends as a function of weight fraction of PH. The  $T_g$ -composition dependence of miscible polymer blends can be accounted for by several theoretical and empirical equations. Of these equations, Gordon–Taylor equation [29] is employed and is written as

$$T_g = T_{g1} + k(W_2/W_1)(T_{g2} - T_{g1}) \quad (1)$$

where  $T_g$  is glass transition temperature of polymer blend,

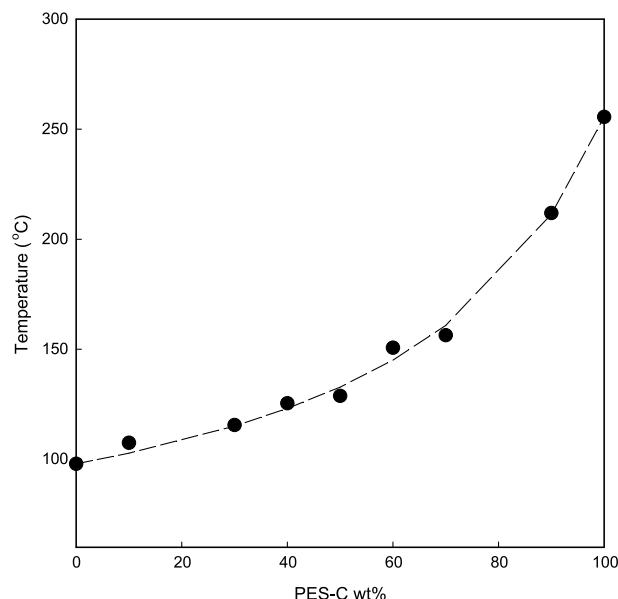


Fig. 3. Plot of glass transition temperature as a function of blend composition for H/PES-C blends. The dash line was drawn from Gordon–Taylor equation with the adjustable parameter  $k = 0.29$ .

and  $T_{g1}$  and  $T_{g2}$  are those of components 1 and 2, respectively.  $W_i$  is the weight fractions and  $k$  is an adjusting parameter related to the degree of curvature of the  $T_g$ -composition diagram. The  $T_g$  prediction by Gordon–Taylor equation fitting to experimental data yielded a  $k$  value of 0.29, fitting the experimental data quite well.

It has been proposed that  $k$  in Eq. (1) can be taken as a semi-quantitative measure of strength of the intermolecular interaction between components of polymer blends [30,31]. For instance, in the blends of poly( $\epsilon$ -caprolactone) (PCL) with chlorinated polyethylene (CPE), poly(vinyl chloride) (PVC) and chlorinated poly(vinyl chloride) (CPVC), the  $k$  values increased from 0.26 to 1.0 with increasing the degree of chlorination, which results from the increase in the amount of the intermolecular hydrogen-bonding between  $\alpha$ -H of the chlorinated polymers and carbonyls of PCL.

Table 1  
Assignment of  $^{13}\text{C}$  CP/MAS spectrum of PES-C

Assignment	Chemical shift (ppm)
1	90
2	118.1
3	119.9
4	123.9
5	125.2
6	126.2
7	129.0
8,9	129.7
10	135.5
11	135.8
12	137.02
13	151.4
14	155.3
15	161.0
16	169.3

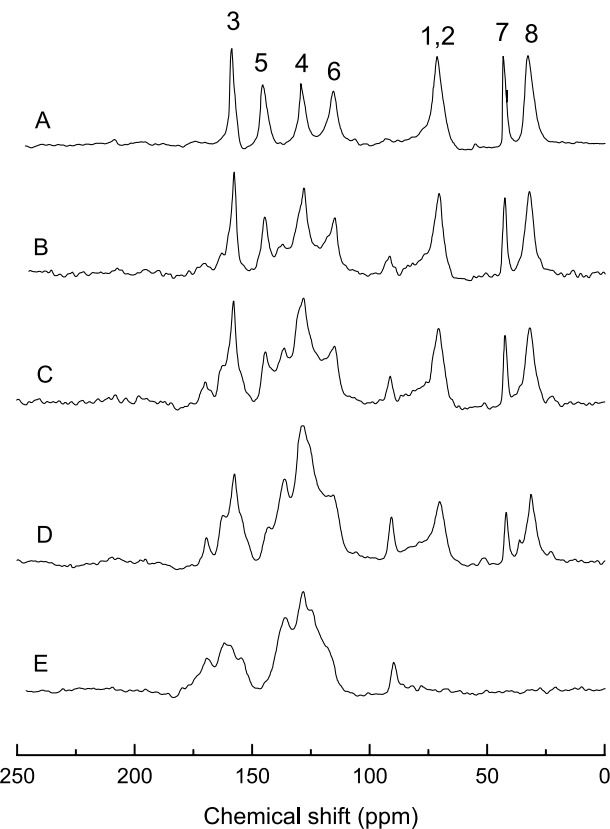
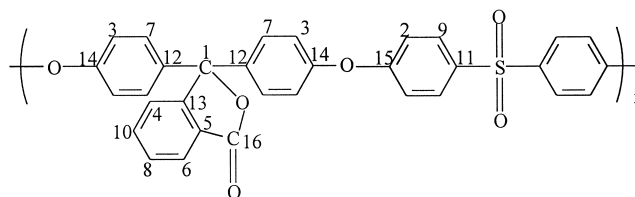


Fig. 4.  $^{13}\text{C}$  CP/MAS spectra of the PH/PES-C blends: (A) 100/0, (B) 70/30, (C) 50/50, (D) 30/70 and (E) 0/100.

When such an approach is used in the PH/PES-C blends, the  $k$  value is 0.29, suggesting that the interaction between PH and PES-C is quite weak.

### 3.1.2. Solid state $^{13}\text{C}$ CP/MAS NMR spectroscopy

**3.1.2.1.  $^{13}\text{C}$  CP/MAS spectra.** The  $^{13}\text{C}$  CP/MAS spectra of PH, PES-C and their blends are shown in Fig. 4. The assignment of PES-C was made with reference of the previous results of the liquid  $^{13}\text{C}$  NMR spectroscopy [32,33] as summarized in Table 1. To confirm the assignment,  $^{13}\text{C}$  CP/MAS experiment using a shorter contact time of 20  $\mu\text{s}$  was performed to obtain the resonance lines of protonated carbons. In the meantime, the dipolar dephasing experiment [32] was conducted to eliminate CH and  $\text{CH}_2$  resonance leaving the resonance lines of quaternary carbons. The pulse sequence was shown in Fig. 1(b), and the dephasing time was 50  $\mu\text{s}$  (Fig. 5).



Phenolphthalein poly(ether sulfone) (PES-C)

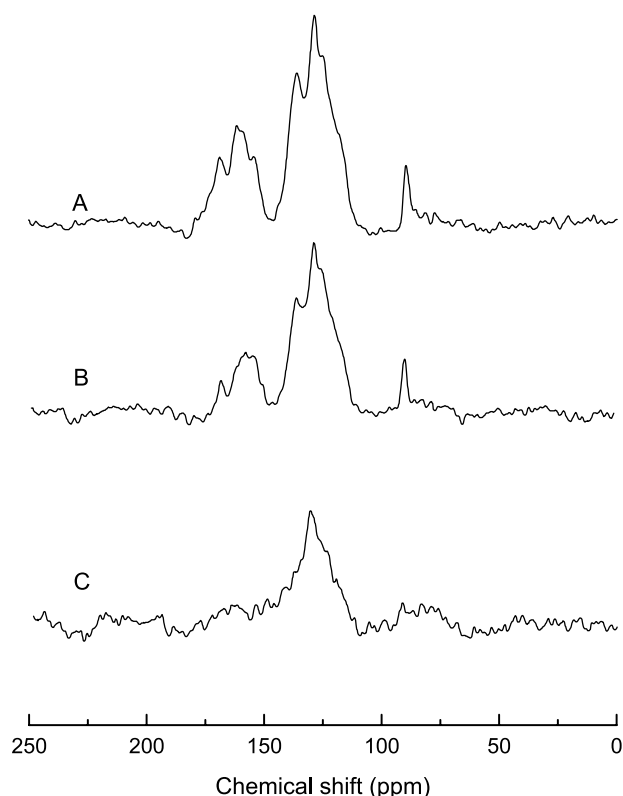
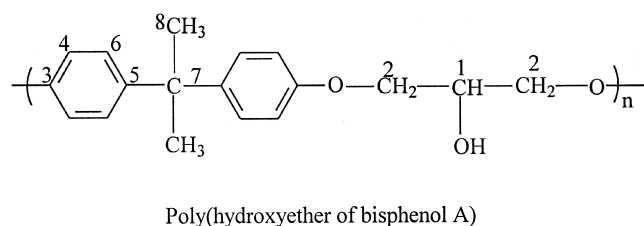


Fig. 5.  $^{13}\text{C}$  CP/MAS spectra of PES-C: (A) 1.0 ms contact time, (B) 50  $\mu\text{s}$  interrupted decoupling with contact time of 1.0 ms, (C) short contact time of 20  $\mu\text{s}$ .

The assignment of the resonance lines of PH was shown as follows [34,35]:



It is seen that from Fig. 4, the spectrum of each PH/PES-C blend can basically be taken as the superposition of the spectra of the pure components. Our attention was focused on the carbonyl group (C-16, 169 ppm) of PES-C, which is potential to form intermolecular hydrogen bonding with the hydroxyl groups of PH. Careful comparison showed no significant changes in the chemical shift of the resonance carbons, suggesting that the intermolecular hydrogen bonding interactions in the blend system are not sufficiently strong to change the chemical shield environment of carbonyl carbon of PES-C.

**3.1.2.2.  $T_{1\rho}(\text{H})$  analysis.** In terms of spin-diffusion mechanism, the protons of the chemically different chains in miscible polymer systems can be closely coupled and

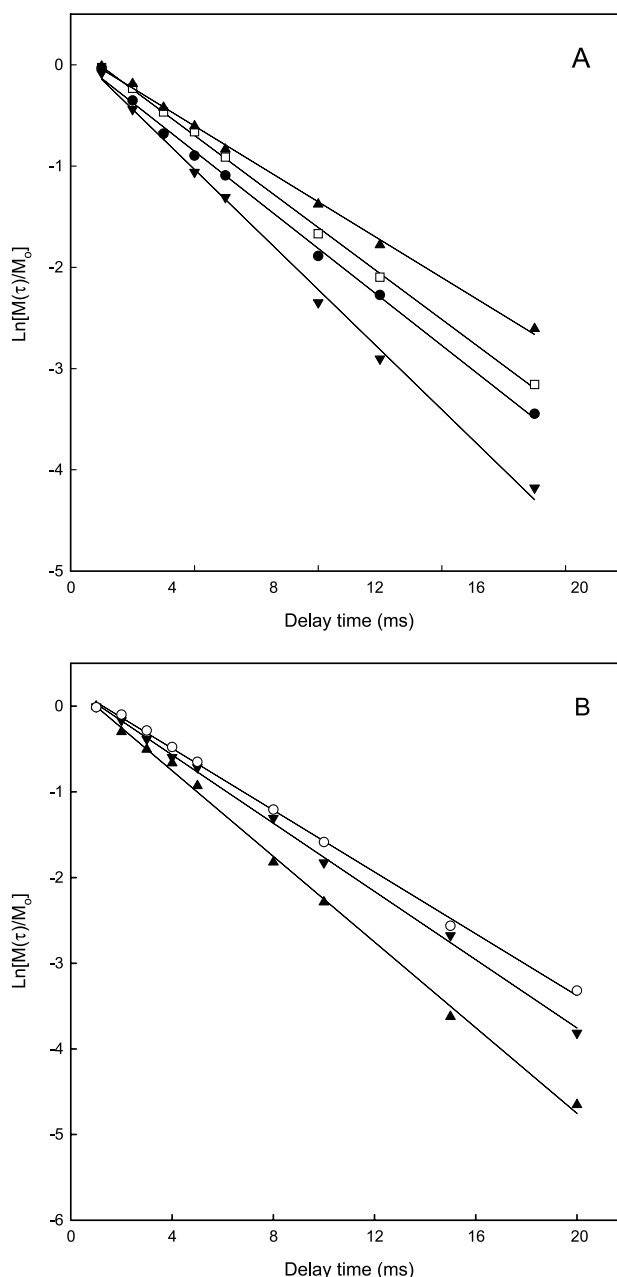


Fig. 6. Logarithmic plot of  $^{13}\text{C}$  CP/MAS resonance intensity versus spin-lock time of PH/PES-C blends for  $T_{1\rho}(\text{H})$  measurement at 32 ppm (A) and 169 ppm (B). (A) (▼) 100/0, (●) 70/30, (□) 50/50, (▲) 30/70. (B): (▲) 0/100, (▼) 30/70, (○) 50/50.

relaxed with an identical rate. In order to examine the homogeneity of the PH/PES-C blends at the molecular level, the spin–lattice relaxation experiment in the rotating frame was carried out using spin-locking pulse sequence. In the spin locking experiment,  $T_{1\rho}(\text{H})$  values can be determined using the exponential function model:

$$M(\tau) = M_0 \exp(-\tau/T_{1\rho}) \quad (2)$$

where  $M(\tau)$  is the intensity of resonance;  $T_{1\rho}(\text{H})$  is the relaxation time in the rotating frame. Fig. 6 representatively shows the logarithmic plots of  $^{13}\text{C}$  CP/MAS resonance



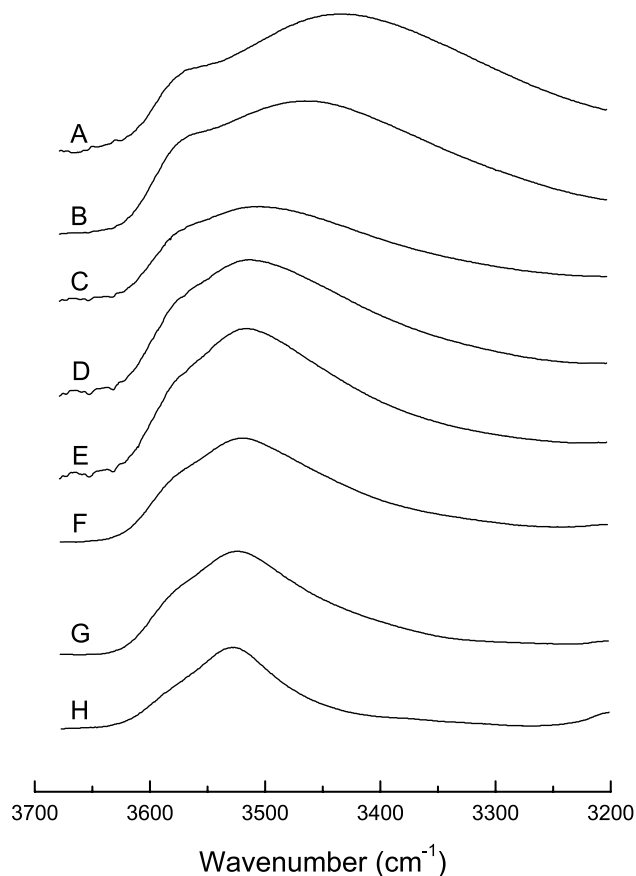


Fig. 7. FTIR spectra of PH/PES-C blends in the region of 3200–3700  $\text{cm}^{-1}$ . (A) PH; (B) 90/10; (C) 70/30; (D) 60/40; (E) 50/50; (F) 40/60; (G) 30/70; (H) 10/90.

intensity  $M(\tau)$  versus delay time at the carbon resonance without overlapping (at 32, 169 ppm) for PES-C, PH and their blends. The fitting of the experimental data with the single exponential decay function is quite well, and the  $T_{1\rho}(\text{H})$  values were determined as summarized in Table 2. The single  $T_{1\rho}(\text{H})$ 's were obtained for each blend, which were intermediate between the relaxation times of the two pure polymers. Within the experimental errors, the  $T_{1\rho}(\text{H})$  values observed at all the carbon are accepted to be identical. The result indicates that fast spin diffusion was carried out among all the protons in these blends, which averaged out of the whole relaxation process, i.e. the

blends are homogeneous on the scale where the spin diffusion occurs within the times  $T_{1\rho}(\text{H})$ 's. The mixing scale can be estimated using the following equation [36–39]

$$L = (6DT_i)^{1/2} \quad (3)$$

where  $D$  is the spin-diffusion coefficient depending on the average proton to proton distance as well as dipolar interaction; it has typically a value of the order of  $10^{-16} \text{ m}^2 \text{ s}^{-1}$ .  $T_i$  is relaxation time ( $T_{1\rho}(\text{H})$ ) from the relaxation experiment. On the basis of  $T_{1\rho}(\text{H})$ 's, the average diffusive path length was calculated to be 20–30 Å, viz. the domain size of the blends is on the scale of 20–30 Å. Therefore, the PH/PES-C blends are judged to be miscible at the molecular level.

### 3.1.3. Fourier transform infrared spectroscopy

The presence of side ester carbonyls gives the potential of PES-C forming the intermolecular specific intermolecular interactions with the hydroxyls of PH via hydrogen-bonding ( $>\text{C}=\text{O} \cdots \text{H}-\text{O}$ ), which are readily detected by means of infrared spectroscopy. PH is a typically self-associated polymer due to the presence of its pendent hydroxyls in the molecular backbone. Addition of PES-C to system could give rise to the break of the self-associated hydrogen bonds of PH, whereas the intermolecular hydrogen bonds will be formed between the chemically different chains to some degree. Shown in Fig. 7 are FTIR spectra of PH and its blends with PES-C in the region of 3200–3700  $\text{cm}^{-1}$ . In this frequency region, the spectroscopic bands are ascribed to the hydroxyl stretching vibration. For the pure PH, the very broad band was attributed to self-associated hydroxyls and the width of the band reflects the wide distribution of hydrogen-bonded hydroxyl stretching frequencies. The shoulder bands centered at 3569  $\text{cm}^{-1}$  are ascribed to the stretching vibration of free hydroxyls. For the PH/PES-C blends, the broad hydrogen-bonded hydroxyl bands are observed to shift to higher frequencies with increasing PES-C concentration. The shift of the hydrogen-bonded hydroxyl stretching bands to the higher frequencies is due to the balance between the number of the strong  $-\text{OH} \cdots \text{OH}$  hydrogen bonds broken and the number of the weaker  $-\text{OH} \cdots \text{O}=\text{C}<$  hydrogen bonds formed,

Table 2

Proton spin–lattice relaxation time  $T_{1\rho}(\text{H})$  (ms) of PH, PES-C and their blends in the laboratory frame

PH/PES-C	PES-C (169 ppm)	PES-C, PH (157 ppm)	PES-C (154 ppm)	PH (144 ppm)	PES-C (136 ppm)	PES-C, PH (129 ppm)	PH (114 ppm)	PES-C (91 ppm)	PH		
									69 ppm	42 ppm	31 ppm
100/0		2.90		2.86		2.89	2.82		2.84	2.86	2.87
70/30	ND	4.23	ND	3.82	ND	3.82	4.54	4.70	3.65	3.90	3.68
50/50	4.20	4.31	ND	ND	4.31	4.66	4.81	5.71	4.48	4.39	4.42
30/70	5.41	4.80	ND	ND	4.99	4.95	ND	5.98	4.82	4.54	4.83
0/100	6.30	6.50	6.40		6.41	6.40		6.22			

Accuracy is  $\pm 5\%$ . ND: not detected due to low ratio of signal to noise.

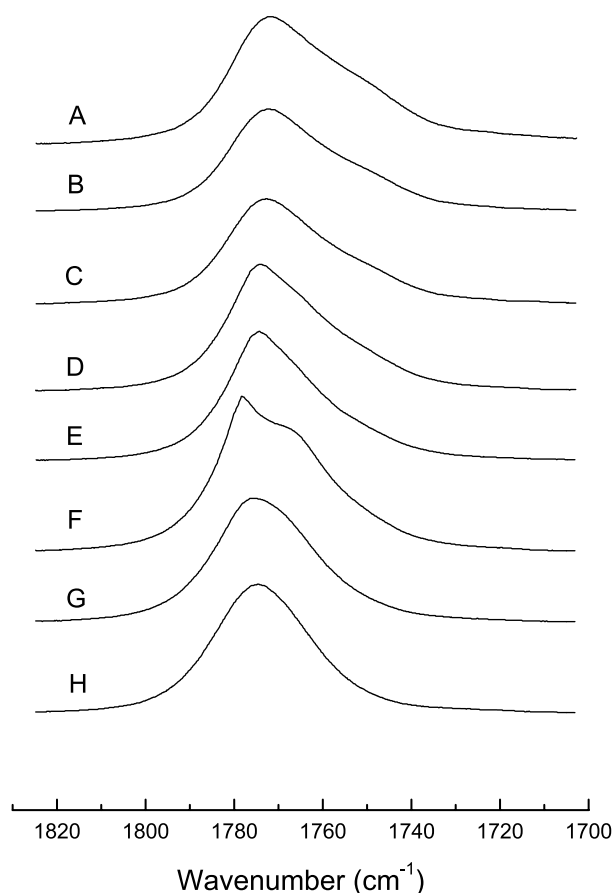


Fig. 8. FTIR spectra of PH/PES-C blends in the range of 1700–1825  $\text{cm}^{-1}$ . (A) 90/10; (B) 70/30; (C) 60/40; (D) 50/50; (E) 40/60; (F) 30/70; (G) 10/90; (H) PES-C.

suggesting that the intermolecular hydrogen bonding strength of the PH/PES-C blends is weaker than that self-association for pure PH [40].

Fig. 8 shows the FTIR spectra of carbonyl stretching vibration in the range of 1700–1830  $\text{cm}^{-1}$  for PES-C and its blends with PH. PES-C is characterized by the band centered at 1778  $\text{cm}^{-1}$  (see curve H). Upon mixing with

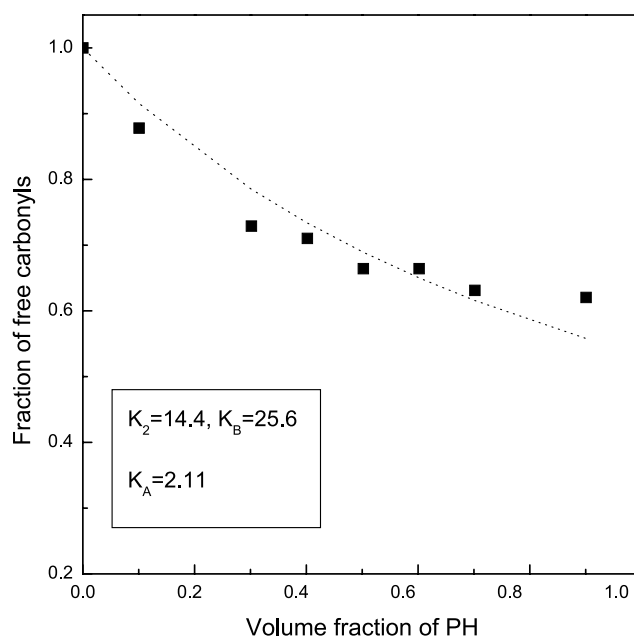


Fig. 9. Fraction of non-associated carbonyl groups of PES-C as a function of blend composition. (■) Experimental data, (---) theory values fit by Eq. (5) with the  $K_A$  of 2.11.

PH, the shoulder centered at the lower frequency of 1753  $\text{cm}^{-1}$  were observed in all the PH/PES-C blends, indicating the formation of the intermolecular hydrogen-bonding involving the carbonyl group of PES-C and hydroxyl group of PH. The shoulder bands could be ascribed to the stretching vibration of the hydrogen-bonded carbonyls. It is possible to resolve the non-associated and the associated carbonyl bands using spectral curve fitting method. The Gaussian line shape function was used in this fitting procedure. The good fitting was carried out for PES-C and the blends and the curve-fitting results were summarized and listed in Table 3. The  $F_{(\text{CO})}^f$  is the fraction of the non-associated carbonyl bands, calculated from the values of absorbency for the associated and the non-associated band contributions

$$F_{(\text{CO})}^f = \frac{A_f}{A_f + (\epsilon_f/\epsilon_a)A_a} \quad (4)$$

Where  $\epsilon_i$  is the molar absorption coefficient. The subscripts,  $f$  and  $a$  stand for free and associated carbonyl groups, respectively. To carry out this calculation, we require the knowledge of the molar absorption coefficients ( $\epsilon_f$  and  $\epsilon_a$ ) or their ratio ( $\epsilon_f/\epsilon_a$ ) for the non-associated and associated carbonyl bands. Using the  $\epsilon_f/\epsilon_a$  value of 1.3 for the interassociation of ester type carbonyls with the hydroxyls of PH blends determined by Coleman et al. [40,48], we calculated the fraction of non-associated carbonyl bands. The variation of  $F_{(\text{CO})}^f$  as a function of the composition is shown in Fig. 9. Using the equations describing the stoichiometry of the system, it has been shown [40] that the  $F_{(\text{CO})}^f$  is related to the equilibrium constants,  $K_2$ ,  $K_B$

Table 3  
Curve fitting results for the PH/PES-C blends at 25 °C

PH/PES-C	Free >C=O bands			Hydrogen-bonded >C=O bands			$F_{(\text{CO})}^f$ (%)
	$\nu$ ( $\text{cm}^{-1}$ )	$W$ ( $\text{cm}^{-1}$ )	$A_f$	$\nu$ ( $\text{cm}^{-1}$ )	$W$ ( $\text{cm}^{-1}$ )	$A_a$	
90/10	1772	18	0.68	1752	19	0.32	62
70/30	1774	18	0.69	1753	19	0.31	63
60/40	1774	18	0.72	1753	19	0.28	66
50/50	1775	18	0.72	1753	19	0.28	66
40/60	1777	18	0.77	1753	19	0.23	72
30/70	1778	18	0.76	1755	19	0.24	71
10/90	1778	18	0.89	1756	19	0.11	87
0/100	1778	18	1.0	—	—	—	100

$\nu$ , wavenumber;  $W$ , bandwidth at the half height of peak;  $A$ , real area fraction.

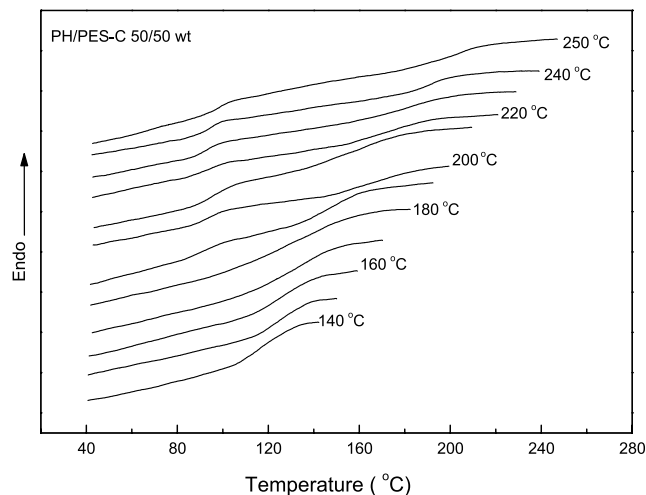


Fig. 10. DSC thermograms of PH/PES-C 50/50 blend at various annealing temperatures between 140 and 250 °C. The annealing time was 10 min.

(self-association) and  $K_A$  (interassociation) through Eq. (5)

$$F_{(CO)}^f = \frac{1}{1 + K_A \Phi_B [(1 - K_2/K_B) + (K_2/K_B)(1/(1 - K_B \Phi_B))]} \quad (5)$$

where  $\Phi_B$  is the volume fraction of isolated (non-hydrogen bonded) B species in the mixture. The value of  $K_A$  is usually determined from a least square fit of Eq. (5) to experimental  $F_{(CO)}^f$  data acquired from mixtures of various compositions. Herein, the values of self-association equilibrium constants,  $K_2$  and  $K_B$  were taken as 14.4 and 25.6, respectively, which were determined for poly(hydroxyether of bisphenol A) by Ilarduya et al. [49]. A value of  $K_A = 2.11$ , is obtained. It is noted that the  $K_A$  is significantly smaller than the  $K_2$  and  $K_B$ , i.e. the self-association is much favored over interassociation. This result is in a good agreement with the observation that the hydroxyl stretching bands of PH shifted to higher frequencies upon adding PES-C to system, indicating that the intermolecular hydrogen bonding between PH and PES-C is weaker than the self-associated of PH. It is the weaker interassociation that could prefigure the potential demixing of the blends at elevated temperature, e.g. LCST behavior.

### 3.2. Behavior of lower critical solution temperature

At elevated temperature, the PH/PES-C blends underwent phase separation. The phase separation was investigated by means of DSC. The homogeneous blend samples were annealed at the upper temperature for 10 min and then quenched 0 °C to re-scan up to a higher temperature. The temperature interval was changed by 10 °C. The annealing temperature corresponding to the first appearance of two separate  $T_g$ 's (or obvious broadening of glass transition) was taken as the phase separation boundaries. Herewith, the results of the PH/PES-C 50/50 (wt) blends were representatively described based on the evolution of thermal properties

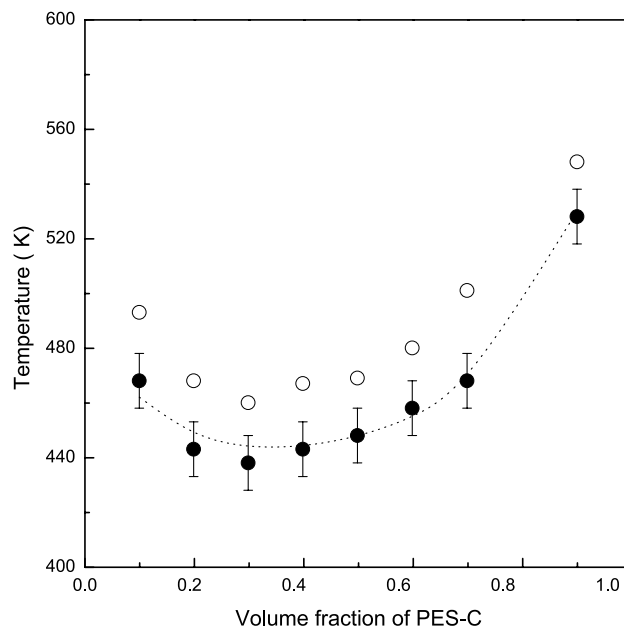


Fig. 11. Phase diagram of PH/PES-C blends: (●) the de-mixing temperatures determined by DSC; (○) the cloud points determined by optical microscopic observation. The dashed line was drawn by best fitting the DSC data on the basis of calculation using Eq. (6).

with annealing temperatures. A series of thermograms were obtained after annealed at temperatures between 140 and 250 °C and then quenched to 0 °C (Fig. 10). It can be seen that the significant change occurred as the annealing temperature exceeds 170 °C, i.e. the glass transition of the blends became broader when annealed at 170 °C for 10 min. The broadening of glass transition may reflect the magnitude of local compositional fluctuations in the polymer blends, implying the relative homogeneity or miscibility of the system. Thereafter, the DSC traces apparently displayed two separate  $T_g$ 's, which were ascribed to those of PH- and PES-C-rich phases, respectively. The appearance of two  $T_g$ 's is indicative of phase separation. The temperature of phase separation was taken as 175 °C. With the phase separation occurring, the  $T_g$  of PES-C-rich phase gradually shifted to higher temperature. Fig. 11 is the plot of the phase boundaries as a function of the blend composition. It was seen that the phase diagram is asymmetrical and has a minimum around 30 wt% PES-C, i.e. the blends display the typical LCST behavior. It can be seen that the de-mixing temperatures determined by optical microscopic observation were higher than those determined by thermal analysis. It is plausible to think that in the blends, the increase in temperature decreases the favorable intermolecular interaction, which in turn results in phase separation.

To estimate the intermolecular interaction parameter of the blend system, Flory–Huggins equation was applied, as written in Eq. (6) [41,42]

$$\Delta G_m = RT \left( \frac{\Phi_1}{V_1} \ln \Phi_1 + \frac{\Phi_2}{V_2} \ln \Phi_2 \right) + A_{12} \Phi_1 \Phi_2 \quad (6)$$



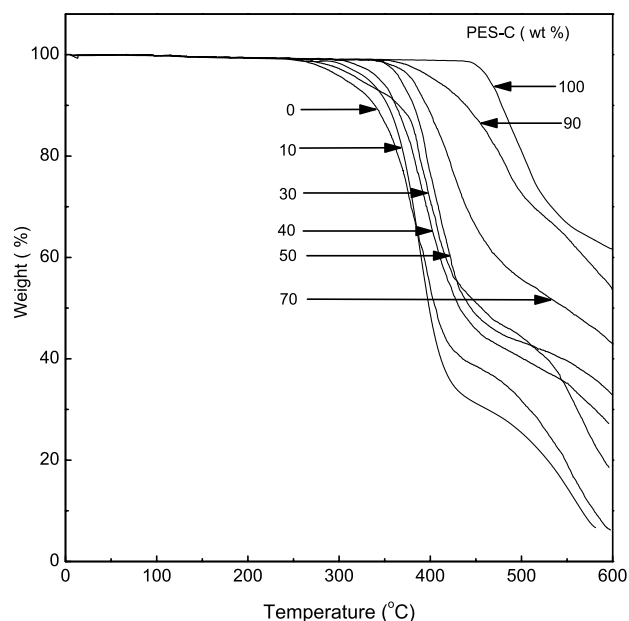


Fig. 12. TGA curves for PH/PES-C blends heated at 10 °C/min.

where  $\Delta G_m$  is the free energy of mixing per unit volume of the mixture;  $V_1$  and  $V_2$ , the molar volumes;  $\phi_1$  and  $\phi_2$  are the volume fraction of the components. The first term in Eq. (6) is the contribution of combinatory entropy to the free energy of mixing. The second term contains  $\Delta_{12}$ , the interaction energy density, which includes all the other contributions to the free energy of mixing that are not accounted for by the combinatorial entropy of mixing represented in the first term.  $\Delta_{12}$  is related to pressure, temperature and composition; in some polymer blends the composition dependence was found to be small [43]. Assuming that the  $\Delta_{12}$  has the dependence on temperature and composition in the following form [44,45]

$$\Delta_{12} = \lambda_0 + \lambda_1 \phi_1 + \lambda_T T \quad (7)$$

where  $\lambda_0$ ,  $\lambda_1$ , and  $\lambda_T$  are constants, which can be determined from the above phase boundaries obtained by means of a non-linear least square fit method. In this work, the values of  $\lambda_0$ ,  $\lambda_1$ , and  $\lambda_T$  were obtained to be  $-1.0881$ ,  $-0.0367$  and  $3.324 \times 10^{-3} \text{ cal cm}^{-3} \text{ K}^{-1}$ , respectively. In this calculation, the weight fractions were converted to volume fractions by dividing the densities of PH and PES-C. The densities of PH and PES-C are 1.252 and 1.262 g/cm<sup>3</sup>, respectively, estimated by a group contribution method [46]. It is seen that the calculated binodal line fits with the experimental demixing temperature points quite well. The interaction energy density ( $\Delta_{12}$ ) is  $-0.1216 \text{ cal cm}^{-3}$  at room temperature (25 °C) and the critical point was found to be 0.29 at 170 °C. The negative value of  $\Delta_{12}$  implies the miscibility of the blend system at room temperature, and the smaller absolute value of interaction parameters also suggests that the intermolecular interaction in the blends is quite weak.

### 3.3. Thermogravimetry analysis

TGA measurement was applied to evaluate the thermal stability of the blends. Fig. 12 shows the TGA scans recorded in air. It was seen that the two pure polymers together with their blends exhibited two-step weight loss mechanism. Obviously, PES-C is more thermally stable than PH. However, no apparently separate weight loss step was seen for the blends, corresponding to the initial degradation of the pure components. This phenomenon could be attributed to the synergistic contribution of the two phases in energy transportation. It was observed that the onset temperatures of the blends increase with increase of PES-C concentration, and the blends exhibited an intermediate thermal stability between those of PES-C and PH. For the PH- and PES-C-rich blends, the onset temperature increase rapidly with increase of PES-C content, however the thermal degradation temperatures change modestly for the blends with the mid-composition. Similar results were obtained for PC/PCL blends by Cheung and Stein [47].

## 4. Conclusions

The miscibility and phase behavior in blends of PES-C and PH were investigated by DSC, solid state <sup>13</sup>C NMR and FTIR. The blends are completely miscible in the entire composition. The glass transition temperatures ( $T_g$ 's) of the blends fit Gordon–Taylor equation quite well, yielding an adjusting parameter of 0.29, suggesting relatively weak intermolecular interactions. FTIR investigation showed that there were the intermolecular hydrogen-bonding interactions between both components, however the inter-association was much weaker than that of self-association of PH. To examine the homogeneity of the blends, the proton spin–lattice relaxation times in the rotating frame  $T_{1\rho}(\text{H})$  were measured via <sup>13</sup>C CP/MAS NMR spectroscopy as functions of blend compositions. In view of the  $T_{1\rho}(\text{H})$  values, it is concluded that the PH and PES-C chains are intimately mixed on the scale of 20–30 Å. At higher temperature, the PH/PES-C blends underwent phase separation, i.e. the blends display the LCST behavior. The phase boundaries were determined by means of thermal analysis, and an asymmetrical phase diagram was established. Based on the phase diagram, the overall interaction energy density ( $\Delta_{12}$ ) was estimated. A small absolute value of interaction parameters suggests that the intermolecular interaction in the blends is quite weak. TGA showed that the blends exhibited improved thermal stability, which increases with increasing PES-C content.

## Acknowledgements

The research grant RGC HKUST6120/99P is acknowledged. One of the authors (S. Zheng) would like to thank the

financial support from Shanghai Science and Technology Commission, China under a Key Project (No. 02DJ14048). One of the authors (Q. Guo) also wishes to express his appreciation to the Natural Science Foundation of China for award to Outstanding Young Scientists (No. 59525307).

## References

- [1] Olabisi O, Robeson LM, Show MT. Polymer–polymer miscibility. New York: Academic Press; 1979.
- [2] Utracki LA. Polymer blends and alloys. New York: Hanser; 1989.
- [3] McBrierty VJ, Packer KJ. Nuclear magnetic resonance in solid polymer. Cambridge, UK: Cambridge University Press; 1993.
- [4] Komoroski RA, editor. High resolution NMR spectroscopy of synthetic polymer in bulk. Deerfield Beach, FL: VCH Publisher; 1986.
- [5] McBrierty VJ, Douglass DC, Kwei TW. *Macromolecules* 1978;11:1265.
- [6] Stejskal EO, Schaefer J, Sefcik MD, McKay R. *Macromolecules* 1981;14:275.
- [7] Dickinson LC, Yang H, Chu CW, Stein RS, Chien CW. *Macromolecules* 1987;20:1757.
- [8] Grobelny J, Rice DM, Karasz FE, MacKnight WJ. *Polym Commun* 1990;31:86.
- [9] Grobelny J, Rice DM, Karasz FE, MacKnight WJ. *Macromolecules* 1990;23:2139.
- [10] Masson JF, Manley RSJ. *Macromolecules* 1992;25:589.
- [11] Schenk W, Reichert D, Schneider H. *Polymer* 1990;31:329.
- [12] Zhang X, Takagoshi K, Hikichi K. *Polymer* 1992;33:712.
- [13] Feng H, Feng Z, Shen L. *Polymer* 1993;34:2516.
- [14] Zhang X, Takegoshi K, Hikichi K. *Macromolecules* 1991;24:5756.
- [15] Belfiore LA, Lutz TT, Cheng C. Solid state NMR of polymer. New York: Plenum Press; 1991. p. 145.
- [16] Liu KL, Zhang HC, Chen TL. Chinese Patent CN8,510,117,211; 1985.
- [17] Zhang Z, Zeng H. *Polymer* 1993;34:4032.
- [18] Guo Q, Qiu L, Ding M, Feng Z. *Eur Polym J* 1992;28:481.
- [19] Guo Q. *Eur Polym J* 1992;28:1049.
- [20] Zhang Z, Zeng H. *Eur Polym J* 1993;29:1647.
- [21] Zheng S, Huang J, Li Y, Guo Q. *J Polym Sci, Part B: Polym Phys* 1997;35:1383.
- [22] Guo Q. *Polymer* 1993;34:70.
- [23] Schulz AR, Young AL. *Macromolecules* 1980;13:633.
- [24] Bank M, Leffingwell J, Ties C. *J Polym Sci, Part A: Polym Chem* 1972;10:1079.
- [25] Djordjevic MB, Porter RS. *Polym Engng Sci* 1977;22:706.
- [26] Robard A, Patterson D, Delmas G. *Macromolecules* 1977;10:706.
- [27] Pearce EM, Kwei TK, Min BY. *J Macromol Sci, Chem* 1984;A21:1181.
- [28] Zheng S, Huang J, Li J, Guo Q. *J Appl Polym Sci* 1998;69:675.
- [29] Gordon M, Taylor JS. *J Appl Chem* 1952;2:495.
- [30] Belorgey G, Prud'homme RE. *J Polym Sci, Polym Phys Ed* 1982;20:191.
- [31] Belorgey G, Aubin M, Prud'homme RE. *Polymer* 1982;23:1051.
- [32] Jin X, Wang F, Liu K. *Fenxi Huaxue* 1989;17:409.
- [33] Wang J, Zhang J, Li B, Feng Z. *Acta Polym Sinica* 1996;June(3):286.
- [34] Zheng S, Guo Q, Mi Y. *J Polym Sci, Part B: Polym Phys* 1998;36:2291.
- [35] Lau C, Zheng S, Zhong Z, Mi Y. *Macromolecules* 1998;31:7291.
- [36] Shaefer J, Stejskal EO. *J Chem Soc* 1976;98:1031.
- [37] McBrierty VJ, Douglass DC. *J Polym Sci, Macromol Rev* 1981;16:295.
- [38] McBrierty VJ, Douglass DC. *Phys Rep* 1980;63:6.
- [39] Tonelli AE. *Macromolecules* 1979;12:255.
- [40] Coleman MM, Graf JF, Painter PC. Specific interaction and the miscibility of polymer blends. Lancaster, PA: Technomic; 1991.
- [41] Roe RJ, Zin WC. *Macromolecules* 1985;18:1609.
- [42] Han CD, Chun SB, Hahn SF, Harper SQ, Savickas PJ, Meunier DM, Li L, Yalcin T. *Macromolecules* 1998;31:394.
- [43] Maruta J, Ougizawa T, Inoue T. *Polymer* 1988;29:2056.
- [44] Roe RJ, Zin WC. *Macromolecules* 1980;13:1221.
- [45] Li JL, Roe RJ. *Polymer* 1988;29:1227.
- [46] Van Krevelen DW, Hoftyzer PJ. Properties of polymer, 2nd ed. Amsterdam: Elsevier; 1980.
- [47] Cheung YW, Stein RS. *Macromolecules* 1994;25:2512.
- [48] Coleman MM, Pehlert GJ, Yang X, Stallman JB, Painter PC. *Polymer* 1996;37:753.
- [49] Ilarduya AM, Eguiburu JI, Espi E, Iruin JJ, Fernandez-Berridi MJ. *Makromol Chem* 1993;194:501.